VHF RADAR IMAGING OF SMALL-SCALE FIELD ALIGNED PLASMA IRREGULARITIES AT LOW, MIDDLE, AND HIGH LATITUDES

D. L. Hysell[1], **H. Bahcivan**[1], **J. L. Chau**[2], **M. F. Larsen**[3], **R. F. Pfaff**[4], **and S. Smith**[5]

(1) Earth and Atmospheric Sciences, Cornell University, Ithaca, NY 14853, USA
(2) Jicamarca Radio Observatory, Instituto Geofísico del Perú, Lima 13, Perú
(3) Physics and Astronomy, Clemson University, Clemson, SC 29634, USA
(4) NASA/Goddard Space Flight Center, Greenbelt, MD 20771, USA
(5) Center for Space Physics, Boston University, Boston, MA 02215, USA

INTRODUCTION

Coherent radar backscatter from field-aligned plasma irregularities is one of the most important means we have for diagnosing the stability of ionospheric regions from the ground and for studying the instability processes at work. Radars provide relatively unambiguous information about the range to the irregularities. Information about the spatial distribution of the irregularities in the transverse directions is more ambiguous; even steerable radars must rely on the stationarity of the target to some extent to construct images of regional irregularity structure, and finite beamwidth effects introduce additional ambiguity, particularly when the targets are spatially intermittent and exhibit high dynamic range. Many radars in use have fixed beams, and the pseudo-images they produce (so-called "range time intensity" images) are only accurate representations to the extent that the flow being observed is frozen-in and lacks important details at scale sizes comparable to or smaller than the scattering volume. It is generally not possible to assess the validity of these assumptions a priori, calling the practice into question.

This paper describes the use of radar interferometry and aperture synthesis imaging to construct high-resolution radar images using fixed-beam coherent scatter radars with arbitrarily broad antenna radiation patterns. True images of the backscatter "brightness" distribution (the distribution of backscatter intensity versus bearing) within the radar illuminated volume can be formed from interferometry data taken with multiple baselines. It is well known that interferometry with a single baseline yields two moments of the brightness distribution. More baselines yield more moments, and a sufficient number of moments define an image in one or two dimensions. (Formally, the interferometry cross spectrum or "visibility" is related to the brightness distribution by an integral transform resembling a Fourier transform.) Radar range gating adds the third spatial dimension. An important feature of in-beam radar imaging that distinguishes it from beam-swinging approaches is that the angular resolution of the technique is limited by the length of the longest interferometry baselines rather than the size of the main antenna array. The former can generally be increased economically whereas the latter generally cannot, and it is possible in practice to form very high resolution images with interferometry even using relatively small radar systems. Images formed from different Doppler spectral components can be combined into composite images, conveying information about the spectral characteristics of different regions of the illuminated volume. In effect, aperture synthesis imaging associates a unique Doppler spectrum with each region in the three-dimensional volume illuminated by the radar.

Imaging methods are inverse methods in that they attempt to invert the brightness-visibility transformation or one related to it. The methods can broadly be categorized as direct or indirect. The former perform the inversion directly, for example by discrete Fourier transform (e.g. the Fourier method), matrix inversion (e.g. SVD), or adaptive filtering (e.g. Capon's method [1]). Such methods may not prove very successful with ill-conditioned or under-determined problems and generally do not consider statistical uncertainties inherent in the data. The latter, meanwhile, select images from families if candidate functions which are consistent with available data but which have other necessary or attractive characteristics. Such methods are generally iterative and work by minimizing a regularization parameter that can incorporate the data, their anticipated statistical uncertainties, and other, prior information (i.e. Bayesian probabilities). The incorporation of prior information permits super-resolution images with granularity better than predicted by the Nyquist sampling theorem.

The radar images presented here were generated using the MAXent algorithm derived from radio astronomy [7]. This is an indirect method that incorporates the Shannon entropy of the image in the regularization

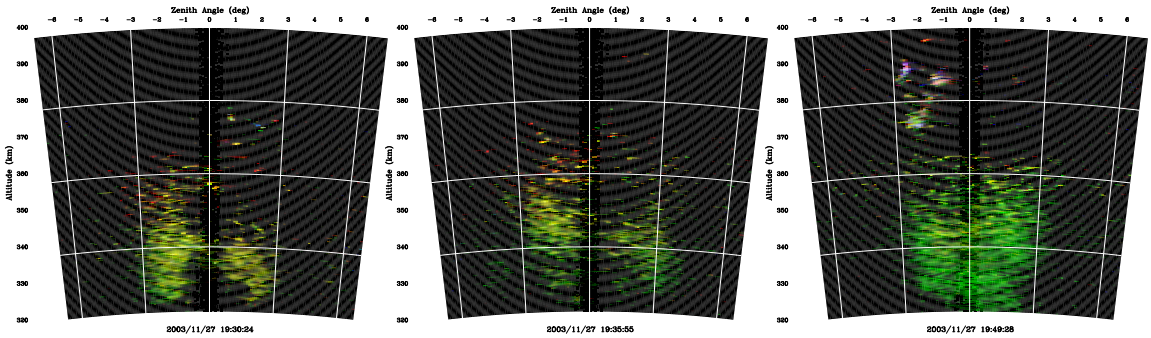

Figure 1: Radar images of a bottom-type scattering layer observed over Jicamarca.

parameter along with the error variances or covariances and which constrains the images to be non-negative. Our purpose is not to describe the algorithm but instead to motivate its application to ionospheric remote sensing and argue its efficacy by two approaches. The first is to recover, through imaging, results that are strongly suspected on the basis of other theoretical or experimental studies. The second and more interesting approach is to observe something new with radar imaging and then validate the discovery by other experimental or theoretical means. Examples will be drawn from observations at low, middle, and high latitudes.

EQUATORIAL IONOSPHERE

Aperture synthesis radar imaging was introduced to the community by [4] to study plasma waves in the equatorial electrojet at the Jicamarca Radio Observatory, and it is there that the technique has undergone the most development. Jicamarca has high-power transmitters and a large, modular phased array antenna which can be subdivided for transmission and reception in a number of configurations. Its data acquisition system supports up to eight receivers. The longest interferometry baseline available for imaging work is approximately 100 wavelengths long. The most commonly used imaging configuration uses 7 receivers supporting 21 nonredundant baselines, the longest being approximately 44 times the shortest.

Imaging has been used at Jicamarca to study equatorial spread *F*, 150 km echoes, the equatorial electrojet, and non-specular meteor trails and has made important contributions in each case. Fig. 1 shows an example of images corresponding to a so-called "bottom-type" scattering layer. These are thin scattering layers that form after sunset in the bottomside *F* region and serve as precursors to fully-developed spread *F*. The images are made with 300 m range resolution, 0.1° zenith angle resolution, and with an incoherent integration time of a few sec. The three images correspond to three different times separated by a few minutes. The brightness of the image pixels represent the signal to noise ratio of the backscatter on a log scale. The hue represents the Doppler shift, with blue and red tones denoting blue and red shifts, respectively. The saturation represents spectral width, with pure and pastel tones denoting narrow and wide spectra, respectively. Echoes are concentrated near the horizontal center of the images because that is the region primarily illuminated by the radar.

[3] recently proposed the theory that the bottom-type layers are composed of horizontal wind-driven interchange instabilities in postsunset bottomside strata where the plasma and neutral zonal drift speeds differ widely and where horizontal plasma density gradients are produced by convection. If so, then the primary plasma waves in the layers should have horizontally elongated and aligned wavefronts rather than vertical wavefronts, as would be expected for Rayleigh Taylor-type instabilities. Radar images like those in Fig. 1 support this theory, showing evidence of primary, kilometer-scale plasma waves with horizontal wavefronts. Confirmation of the [3] helps to explain why the layers remain vertically confined over time, drift in the direction opposite that of the zonal thermospheric wind, and form at altitudes well below where the bottomside vertical plasma density gradient is steepest.

Moreover, the images also demonstrate an unexpected feature of the layers. Fig. 1 shows that the primary plasma waves do not fill the radar illuminated volume but instead often appear to be concentrated into regions (clumps) separated by about 30 km. This clumping only occurs on evenings when fully-developed spread

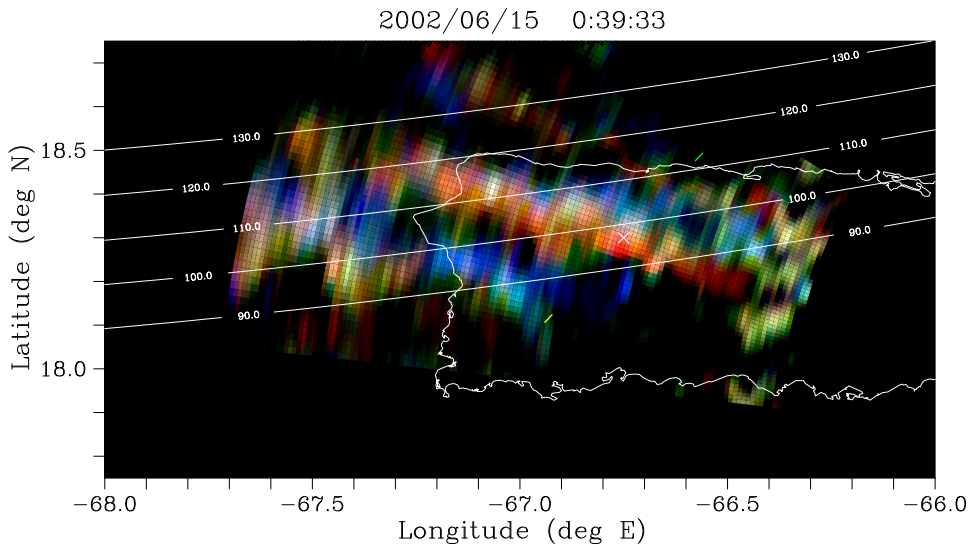

Figure 2: Radar images of a QP echo event observed by a portable 30 MHz radar imager on St. Croix, USVI.

F forms later. We interpret the 30 km periodicity as evidence of large-scale precursor waves in the bottomside. Different phases of the waves would be alternately stable and unstable to wind-driven interchange instabilities. The discovery of the 30 km periodicity and the large-scale precursor waves behind them was validated recently in a NASA sounding rocket campaign carried out from Kwajalein Atoll and has important implications for forecasting spread *F*.

MID-LATITUDE IONOSPHERE

Aperture synthesis imaging can equally well be utilized by compact radars. A portable 30 MHz radar interferometer was deployed in the summer of 2002 to St. Croix in the U. S. Virgin Islands to study sporadic *E* layer irregularities and so-called "QP" echoes in conjunction with the Arecibo Radio Observatory [2]. The 30 MHz radar had a peak power of only 8 kW and 9 nonredundant interferometry baselines, the longest being about 16 wavelengths long. Both radars shared a common volume, with Arecibo able to monitor incoherent scatter where the 30 MHz radar detected coherent scatter. The objective was to associate the QP echo sources with billow-like structures sometimes seen in sporadic *E* layers [5]. Based on interferometric observations of QP echoes carried out earlier, we anticipated that the coherent scatter would arrive from horizontally drifting, patchy regions of space drifting through the radar beam [8, 6]. We expected these patchy regions to correspond to the billow structures seen by Arecibo.

Fig. 2 shows a snapshot taken from our imaging results on St. Croix. The images were constructed in three dimensions, but the altitude dimension was integrated out in order to facilitate reproduction in print. The actual centroid altitude for the backscatter was between 100–110 km, depending on local time. The altitude matched the height of the sporadic *E* layer detected simultaneously by Arecibo. Furthermore, the individual regions from which coherent scatter was detected were co-located with billow-like structures in the layers seen by Arecibo. In this regard, our expectations were corroborated by radar imaging.

In addition, imaging revealed a tendency for the patchy scattering regions to coalesce and form frontal structures and wavefronts. These wavefronts are clearly evident in the example in Fig. 2. Not only is the backscatter intensity modulated by the wavefront, but also are the Doppler shifts, which alternate between positive and negative extremes in different phases of the large-scale (about 30 km wavelength) wave. As the Doppler shifts are indicative of the $\mathbf{E} \times \mathbf{B}$ drifts of the *E* region electrons, the image suggests the presence of a large-scale electrostatic wave. The waveform propagated to the southwest in this case at about 50 m/s. Remarkably, the same wave-like morphology (wavelength and propagation direction) was detected by the Boston University all-sky imager in its 557.7 nm images when the layer descended to sufficiently low altitudes.

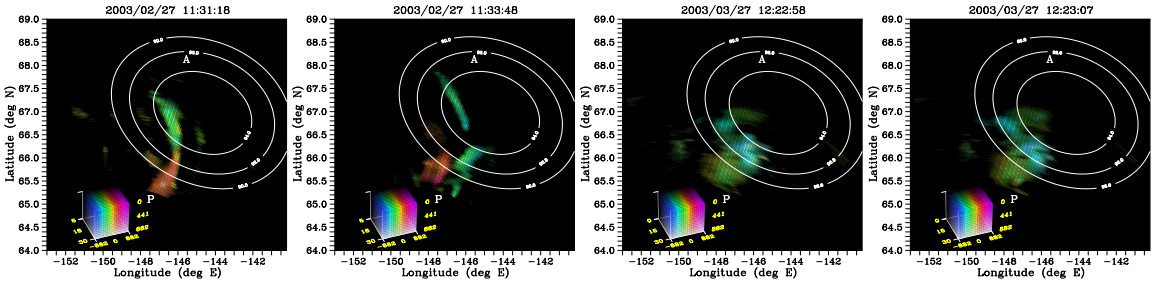

Figure 3: Radar images of the auroral electrojet observed from Anchorage, Alaska.

AURORAL IONOSPHERE

In the spring of 2003, the 30 MHz radar imager was deployed to Anchorage, Alaska to support the NASA JOULE sounding rocket campaign at the Poker Flat Rocket Range. The objective of the campaign was to study small-scale variability in the convection electric field and the contribution this makes to Joule heating. The radar was used as a diagnostic of auroral conditions and also as a means of measuring fine structure in the convection pattern regionally. Evidence of convection features with compact spatial and temporal scales can be inferred from the representative radar images in Fig. 3.

Radar imaging was particularly useful in sorting echoes from different azimuths. The Doppler spectra could vary widely with azimuth angle and would tend to produce complicated, composite spectral forms if combined. Spectra from different regions in the images were meanwhile all of the type I or type II variety. By comparing the spectra with *in situ* measurements of the electric field, it was possible to associate each of the spectra with the underlying electric field. Consistent with expectations, we found that type I echoes have Doppler shifts close to the local ion acoustic speed. Type I echoes were only observed when the convection was in the direction of the radar line of sight (i.e. at zero flow angle), regardless of the convection speed. Defying expectations, however, we also found that all other echoes were type II and exhibited Doppler shifts equal matching the ion acoustic speed times the cosine of the flow angle. This finding is consistent with new results of numerical simulations of Farley Buneman instabilities to be presented by M. Oppenheim at this meeting of the URSI GA.

References

[1] J. Capon. High-resolution frequency-wavenumber spectrum analysis. *Proc. IEEE*, 57:1408, 1969.

[2] D. L. Hysell, M. F. Larsen, and Q. H. Zhou. Common volume coherent and incoherent scatter radar observations of mid-latitude sporadic *E*-layers and QP echoes. *Ann. Geophys.*, 22:3277, 2004.

[3] E. Kudeki and S. Bhattacharyya. Post-sunset vortex in equatorial *F*-region plasma drifts and implications for bottomside spread-*F*. *J. Geophys. Res.*, 104:28,163, 1999.

[4] E. Kudeki and F. Sürücü. Radar interferometric imaging of field-aligned plasma irregularities in the equatorial electrojet. *Geophys. Res. Lett.*, 18:41, 1991.

[5] K. L. Miller and L. G. Smith. Incoherent scatter radar observations of irregular structure in mid-latitude sporadic *E* layers. *J. Geophys. Res.*, 83:3761, 1978.

[6] C. J. Pan, C. H. Liu, J. Röttger, and S. Y. Su. A three dimensional study of *E* region irregularity patches in the equatorial aeronomy region using the Chung-Li VHF radar. *Geophys. Res. Lett.*, 21:1763, 1994.

[7] J. Skilling and R. K. Bryan. Maximum entropy image reconstruction: General algorithm. *Mon. Not. R. Astron. Soc.*, 211:111, 1984.

[8] M. Yamamoto, N. Komoda, S. Fukao, R. T. Tsunoda, and T. Ogawa. Spatial structure of the *E* region field-aligned irregularities revealed by the MU radar. *Radio Sci.*, 29:337, 1994.